Mineralogical Magazine, December 1998, Vol. 62(6), pp. 743–757

Coronas, reaction rims, symplectites and emplacement depth of the Rymmen gabbro, Transscandinavian Igneous Belt, southern Sweden

D. T. CLAESON

Department of Geology, Earth Sciences Centre, Göteborg University, 413 81 Göteborg, Sweden

ABSTRACT

Reactions between olivine and plagioclase form kelyphytic corona textures in the Rymmen gabbro, southern Sweden. The coronas surround olivine and consist of enstatite ± amphibole and phlogopite, combined with an outer rim of symplectic intergrowth of green spinel and amphibole. Corona reactions took place in fractures within olivine prior to the formation of chlorite, serpentine, and magnetite in the fractures at cooler conditions. Disequilibrium between olivine and plagioclase has been put forward as an explanation for the corona formation. However, inclusions of plagioclase in olivine show that there is no reaction between these minerals, since no new minerals formed between them. The conclusion drawn is that the most important factor for development of kelyphytic structures in the Rymmen gabbro is contact with a late deuteric fluid in an environment where olivine and plagioclase are close to each other. Temperature estimates for the formation of the kelyphytic coronas in the Rymmen gabbro yield consistent temperatures of around 800 ± 30°C and pressures 6–8 kbar, which indicate emplacement at a depth of 20–30 km in the crust. Late deuteric fluids caused olivine replacement by intergrown orthopyroxene and magnetite, in Fe-Ti oxide-rich rocks only. In these, plagioclase is replaced by symplectite when in contact with ilmenite and magnetite. It is noted that the symplectite minerals have low Ti contents. This suggests that the Fe-Ti oxide was a catalyst for the reaction between plagioclase and late-stage aqueous fluids rather than being a reactant, alternatively that the magnetite/ilmenite was a reactant and Ti was retained in the oxide.

KEYWORDS: kelyphytic corona, reaction rim, gabbro, ilmenite-magnetite-plagioclase reaction, orthopyroxene-magnetite-pleonaste symplectite, Transscandinavian Igneous Belt.

Introduction

THE formation of coronas, reaction rims and symplectites in rocks indicates a change in chemical and/or physical factors. This could be during a prograde or retrograde metamorphic event, sometimes associated with cooling from igneous temperatures (e.g. Griffin and Heier, 1973; Mongkoltip and Ashworth, 1983). Coronas completly surround a mineral, which has reacted with adjacent minerals, wheras reaction rims are local isolated replacement features (Passchier and Trouw, 1996). The coronas investigated in this study consist of layers of different minerals combined with an outer rim of symplectic intergrowth of green spinel and amphibole, i.e. a kelyphytic structure (Passchier and Trouw, 1996). Symplectites are formed of two or more minerals that are intergrown as lamellae (e.g. Mongkoltip and Ashworth, 1983). The lamellae can be straight, curved or vermicular. Coronas or reaction rims are developed where olivine is in contact with plagioclase.

The aim of this study was to elucidate the formation of coronas, reaction rims and symplectites in the Rymmen gabbro, a layered mafic intrusion in the southern part of the Transscandinavian Igneous Belt (TIB) in Sweden (Fig. 1) and deduce its emplacement

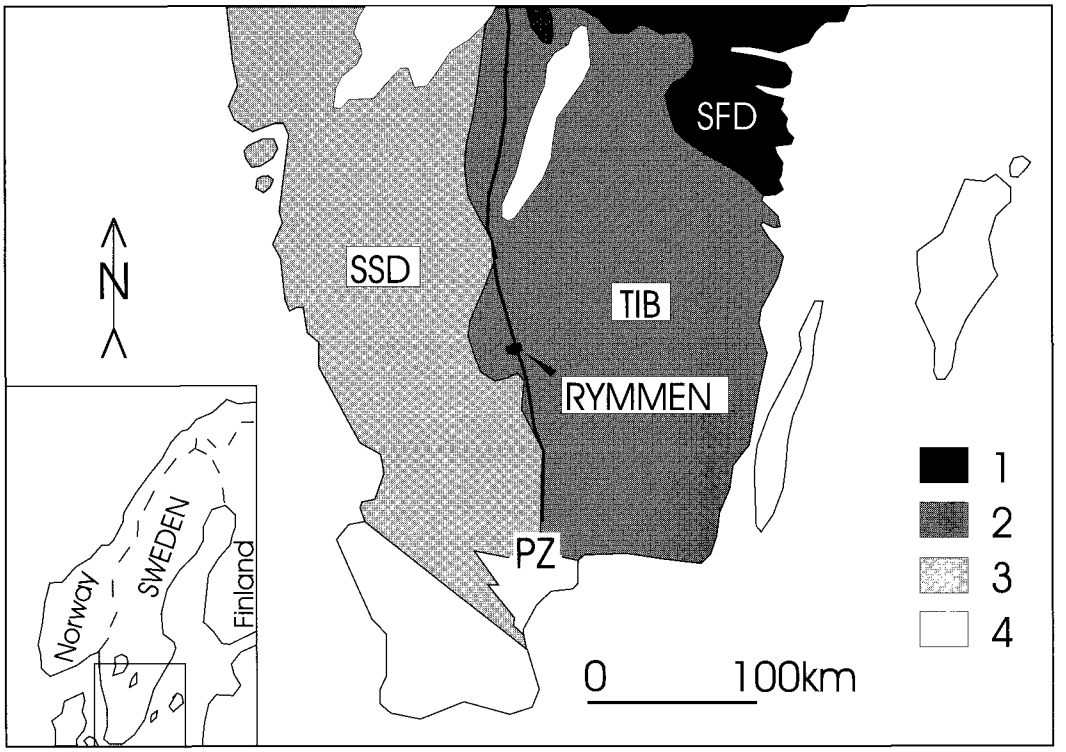

FIG. 1. Sketch map showing location of the Rymmen gabbro (black dot) and tectonic subdivision of southern Sweden. Key: 1, Svecofennian Domain - SFD; 2, Transscandinavian Igneous Belt - TIB; 3, Southwest Scandinavian Domain - SSD; 4, Phanerozoic cover.

depth. Three textures — kelyphytic structures, orthopyroxene-magnetite-pleonaste symplectites, and symplectites formed by reaction between plagioclase and magnetite/ilmenite — are presented in this paper.

Geologic setting

The TIB constitutes a major granitoid complex, extending from the south of Sweden to northern Norway (Gaál and Gorbatschev, 1987; Gorbatschev and Bogdanova, 1993).

The Rymmen gabbro is situated within the Protogine Zone (Gorbatschev, 1980; Fig. 1) and was emplaced during the *c.* 1.7 Ga TIB event, shown by a Pb-Pb age of 1692 ± 7 Ma (2σ) (Claeson in manuscript). It has a compositional range from hornblende leucogabbro to olivine melagabbro (Claeson and Larson, 1996) and modal layering, cryptic layering, igneous textures and primary chemistry are preserved. Folds or penetrative foliation are absent, which demonstrate that deformation has only been minor.

Analytical technique

Polished sections were made for mineral chemical analysis. All minerals were determined at the Earth Sciences Centre, Göteborg University, with a Zeiss® DSM 940 scanning electron microscope (SEM) with a Link® energy dispersive spectrometer (EDS) system. Accelerating voltage of 25 kV, sample current about 1 nA and counting livetime of 100 s were used. Spot analysis of an area of ~50 μm^2 was used on symplectites, except for one which was ~5 μm^2. The setting was the same as that used when calibration on natural minerals and synthetic standards were performed. A cobalt standard was used as reference standard to monitor instrument drift during runs. ZAF correction was utilised. Additional mineral data are available on request from the author.

Kelyphytic structures

Petrography and geochemistry

Kelyphytic coronas or reaction rims between olivine and plagioclase are found in cumulate rocks in the Rymmen gabbro. These rocks have whole-rock magnesium number ($Mg/(Mg+Fe_T)$ = Mg#) between 75 and 79, which shows that they were formed early in the evolution of the intrusion. A prolonged period of recrystallization at elevated temperatures in a static stress field is indicated by the unfoliated texture with 120° triple junctions between plagioclase.

Olivine

Olivines are chrysolite with forsterite contents of 74–80% (Table 1). No zoning was detected. Secondary magnetite and chlorite or serpentine are found within cracks in olivine. Inclusions of olivine are present in amphibole, plagioclase and clinopyroxene. Only minor rims of secondary amphibole or orthopyroxene (Fig. 2*a*) or no reaction at all is found between olivine and magmatic amphibole (Fig. 2*b*). Olivine and plagioclase situated within interstitial magmatic amphibole do not develop a kelyphytic structure if the distance is over 50 μm between the minerals in the plane of the thin-section. The modal content of olivine in the studied samples varies between 6 and 48%.

Plagioclase

The anorthite content of plagioclase varies between 85 and 90% (Table 1) and it is chemically unzoned. Inclusions of plagioclase are found in amphibole and clinopyroxene, and more rarely in olivine, where they are seen as symplectitic spots. The modal content of plagioclase varies between 22 and 82%.

Orthopyroxene

Orthopyroxene is present in two completely different associations, as interstitial magmatic grains and as a layer adjacent to olivine in kelyphytic structures. They are in both cases

TABLE 1. Magmatic mineral analyses from samples with kelyphytic corona developed and coronitic orthopyroxene

Sample	95608 ol36	95608 cpx14	95608 opx37	95070 opx45	95608 plag41	95608 amp34
Na_2O		n.d.			1.33	1.12
MgO	41.81	16.05	30.92	29.25		16.74
Al_2O_3	0.14	2.62	0.63	2.17	34.80	12.41
SiO_2	39.09	53.46	57.16	54.73	46.03	44.48
K_2O					0.00	0.73
CaO	0.02	23.87	0.25	0.97	17.89	12.30
TiO_2		0.56		0.35		2.12
Cr_2O_3		0.50	n.d.	n.d.		0.55
MnO	0.27	0.14	0.40	0.36		0.14
FeO	19.23	4.53	12.28	13.01	n.d.	7.23
NiO	n.d.					0.11
Sum	100.56	101.72	101.65	100.84	100.03	97.94
Mg′	79.3	86.3	81.8	80.1		0.975
Wo		48	0.5	1.9		
En		45	81.4	78.5	An 88.2	
Fs		7	18.1	19.6	Ab 11.8	
Si/Al			76.5	21.5	Or 0.0	
Mineral	olivine	clino-pyroxene	ortho-pyroxene corona	ortho-pyroxene magmatic	plagioclase	ferrian-tscherma-kitic hbl

The program PROBE-AMPH (Tindle and Webb, 1994) was used to determine amphibole name. n.d. = not detected.

enstatite with Mg# 77–81 and are only present in small amounts. No zoning was detected and no exsolution was observed. $Mg/(Mg+Fe_T)$ is always higher than in coexisting olivine. Table 1 gives a representative analysis of orthopyroxene formed in reaction rims adjacent to olivine. The measured width of the orthopyroxene rims is less than 60 μm. These rims are not always developed in the corona formation, only kelyphytic symplectite is present in some samples. In some thin-sections the orthopyroxene rim is in contact with magmatic orthopyroxene grains. Table 1 gives a representative analysis of magmatic orthopyroxene from samples with kelyphytic structures. Orthopyroxene is an interstitial late crystallizing phase in olivine-bearing parts of the intrusion.

Clinopyroxene

Clinopyroxene is found both as an early cumulate phase and late interstitial phase in a single thin-section and never in kelyphytic structures. There are no detectable chemical differences between them. No zoning or exsolution was detected. Table 1 gives a representative analysis of clinopyroxene from a sample with kelyphytic structures. Inclusions of clinopyroxene are present in amphibole, plagioclase and olivine. When plagioclase is present in interstitial clinopyroxene, a thin rim of amphibole usually surrounds the plagioclase.

Amphibole

Amphibole is present as a late interstitial magmatic phase and as a reaction phase within kelyphytic structures. Kelyphitic amphibole develops between the symplectite layer and the orthopyroxene layer. Various amphibole compositions are recognised among the kelyphitic amphiboles as shown in Table 2. The interstitial magmatic amphibole that is observed coexisting with olivine does not invade the space between the orthopyroxene rims and symplectite. An analysis of a magmatic amphibole is presented in Table 1.

Spinel

Pleonaste (green spinel), picotite and chromian magnetite are present as distinct grains in some coronas (Fig. 2*c*; Table 3). Pleonaste is the only spinel that is also present as a symplectic intergrowth with amphibole. Analyses on spinel rods or vermicules from the symplectite showed minor contamination from adjacent amphibole. However, it was concluded that the mineral has the composition $(Mg, Fe)Al_2O_4$. In thin-section the characteristic green colour and its isotropic nature were evident.

Biotite and phlogopite

Biotite and phlogopite are late crystallizing minerals, interstitial in some samples, usually as discrete grains with Mg# between 79 and 87. Phlogopite was found in only one kelyphytic corona (Table 2).

Symplectite in kelyphytic structures

The symplectite in the kelyphytic structures consists of two separate mineral phases, which are amphibole and pleonaste (Table 4). These are intergrown in an intricate web (Fig. 2*c,d*). Maximum symplectic rim width measured in thin-section is around 200 μm. The rim width varies within a single thin-section as well as within a single corona (Fig. 2*d*). Rims are only developed all around the olivine when it is surrounded by plagioclase (Fig. 2*e*), thus forming a corona. Modal content of symplectite ranges from a few percent to 12%.

Orthopyroxene-magnetite-pleonaste symplectites

Olivine is replaced by orthopyroxene-magnetite-pleonaste symplectites (Fig. 3) in an Fe-Ti oxide rich part of the Rymmen gabbro. A whole-rock Mg# of 43 shows that this part of the intrusion is more evolved compared with those parts having kelyphytic structures. This type of symplectite is not seen elsewhere in the intrusion. In transmitted light the symplectites are opaque due to the high content of disseminated magnetite (Zeck *et al.*, 1982) and could therefore only be studied in reflected light. Calculation of the content resulted in 68–80% orthopyroxene, 18–31% magnetite and 1–2% pleonaste for different symplectite analyses (Table 5). The analyses reveal that there is little to no ilmenite present. Pleonaste is found in proper magnetite grains as exsolution lamellae along with ilmenite.

Symplectites between plagioclase and magnetite/ilmenite

In the Fe-Ti oxide rich part of the intrusion, symplectic coronas are developed between Fe-Ti

TABLE 2. Amphibole/phlogopite analyses in kelyphytic coronas

Sample	95585 amp21	95069 amp69	95070 amp34	95070 amp41	95073 mica13a	95075 amp17	95608 amp38
Na_2O	1.96	0.34	1.36	1.55	0.43	1.72	n.d.
MgO	17.56	21.94	15.55	16.97	22.92	16.04	22.20
Al_2O_3	12.78	3.12	12.99	13.16	17.41	13.39	3.03
SiO_2	46.92	56.29	45.12	44.57	39.49	45.23	55.79
K_2O	0.26	n.d.	0.67	0.25	9.76	0.54	n.d.
CaO	12.54	13.17	12.54	11.48	0.05	12.52	12.43
TiO_2	n.d.	n.d.	1.33	0.50	0.17	0.56	n.d.
MnO	0.11	0.07	0.10	0.12	0.01	0.11	0.16
FeO	6.55	3.98	7.60	7.98	6.16	7.47	4.46
Sum	98.69	98.92	97.27	96.58	96.41	97.56	98.07
Struct. formula							
Si	6.508	7.618	6.442	6.307	5.57	6.413	7.589
Aliv	1.492	0.382	1.558	1.693	2.43	1.587	0.411
Alvi	0.597	0.115	0.628	0.502	0.46	0.651	0.075
Ti	n.d.	n.d.	0.143	0.053	0.02	0.060	n.d.
Fe^{3+}	0.596	0.359	0.309	0.944		0.442	0.507
Fe^{2+}	0.164	0.092	0.598	0.000	0.73*	0.444	0.000
Mn	0.013	0.008	0.012	0.014	0.00	0.013	0.018
Mg	3.631	4.426	3.310	3.508	4.82	3.390	4.502
Ca	1.863	1.910	1.918	1.741	0.01	1.902	1.812
Na	0.527	0.089	0.376	0.425	0.12	0.473	n.d.
K	0.046	n.d.	0.122	0.045	1.76	0.098	n.d.
(Ca+Na)(B)	2.00	1.999	2.000	1.906		2.000	1.812
Na(B)	0.137	0.089	0.082	0.165		0.098	n.d.
(Na+K)(A)	0.437	0.000	0.417	0.305		0.473	n.d.
$Mg/(Mg+Fe^2)$	0.957	0.980	0.847	1.000		0.884	1.000
$Fe^3/(Fe^3+Alvi)$	0.500	0.757	0.330	0.653		0.404	0.871
Mineral	magnesio hbl	tremolite	tscherma-kitic hbl	ferrian-tscherma-kitic hbl	phlogopite	tscherma-kitic hbl	tremolite

The program PROBE-AMPH (Tindle and Webb, 1994) was used to determine structural formula and mineral name. Formula on the basis of 23 and 22 oxygen resp.
* All Fe as FeO.
n.d. = not detected.

oxide and plagioclase (Fig. 4*a,b*). These are composed of amphibole and pleonaste, with proportions from 85:15 to 90:10 (Table 6). The anorthite content of plagioclase varies between 72 and 76%. The magnetite has exsolution lamella of both hercynite (Turnock and Eugster, 1962) and ilmenite (Fig. 4*b* and Table 7). The recognition of symplectite that formed between plagioclase and Fe-Ti oxide requires microscopy in reflected light to separate it from the orthopyroxene-magnetite-pleonaste symplectites.

Other reaction rims

In some thin-sections a reaction rim between clinopyroxene and magmatic amphibole is present. The clinopyroxene is rimmed by actinolite or tremolitic-hornblende and bordered by interstitial magmatic tschermakitic-hornblende due to uralitisation (Table 8).

Picotite rimmed by green spinel is found in the basal parts of the intrusion. Similar spinel rims have been described in magnesium rich tholeiites from Adrano, Mt Etna (Kamenetsky and

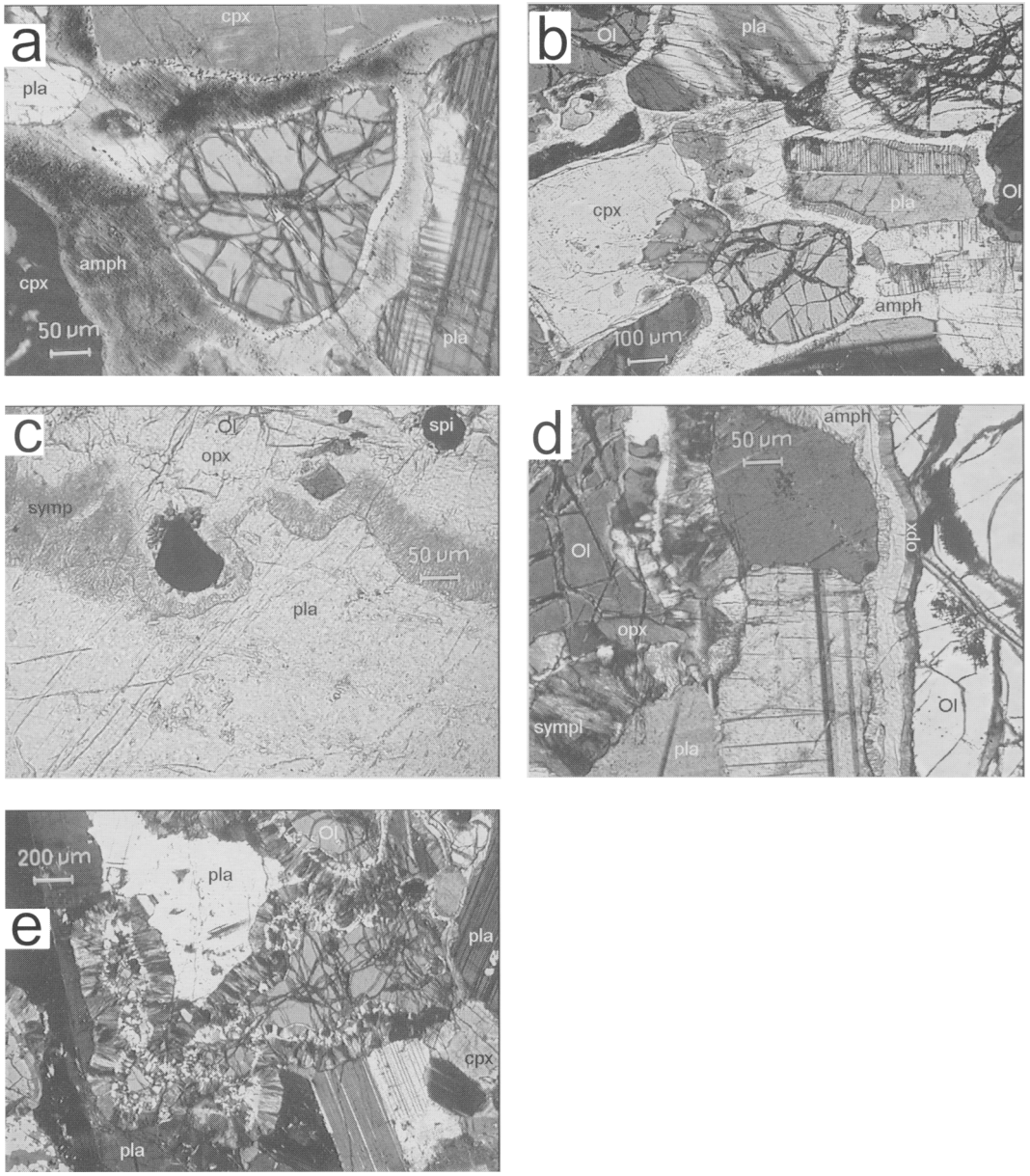

FIG. 2. Features of kelyphytic structures: (*a*) Minor rim of orthopyroxene and a different amphibole compared with the magmatic amphibole. Note that no symplectite or pleonaste has developed in the plagioclase where orthopyroxene is developed in the facing olivine. Crossed polars. (*b*) Olivine showing no reaction with magmatic amphibole when plagioclase is too far away. Note that the cpx is intact and only bordered with magmatic amphibole. Crossed polars. (*c*) Pleonaste or green spinel, picotite and chromian magnetite are present as distinct grains in a corona. The two latter are more chrome rich spinels. Plane-polarized light. (*d*) Symplectic rim intergrown in an intricate web. Note that the rim width varies within a single thin-section as well as within separate coronas. Crossed polars. (*e*) Rims are only developed all around the olivine when it is facing plagioclase in all directions. Crossed polars.

TABLE 3. Spinel grains within kelyphytic coronas

Sample	95585 spi50	95076 spi16	95606 spi29	95606 spi30
Na_2O	0.38	n.d.	n.d.	n.d.
MgO	11.84	12.59	9.05	0.41
Al_2O_3	47.87	55.29	39.60	2.03
SiO_2	5.61	n.d.	n.d.	n.d.
CaO	1.67	n.d.	n.d.	n.d.
TiO_2	n.d.	n.d.	0.04	0.55
V_2O_5	n.d.	n.d.	0.05	0.14
Cr_2O_3	10.83	6.47	18.42	10.67
MnO	n.d.	0.19	0.41	0.20
FeO	24.36	23.53	32.20	79.92
NiO	n.d.	0.15	0.22	0.23
ZnO	n.d.	0.33	n.d.	n.d.
Sum	102.55	98.56	99.99	94.14
Mg′	46.4	48.8	33.4	0.9
Cr′	13.2	7.3	23.8	77.9
Fe/Mg	1.15	1.05	1.99	110
Mineral	pleonaste	pleonaste	picotite	chromian-magnetite

n.d. = not detected.

Clocchiatti, 1996), subduction-related lavas (Della-Pasqua *et al.*, 1995) and ocean-ridge tholeiites (Natland, 1989; Allan *et al.*, 1988).

P–*T* estimations

Kelyphytic corona formation

Pressure estimates for the olivine-plagioclase reaction indicate a depth of around 15–35 km (Table 9).

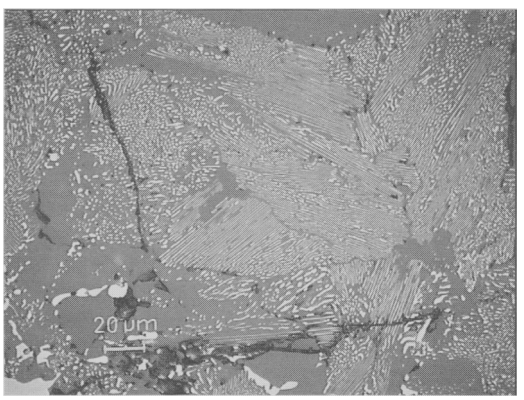

FIG. 3. Olivine is replaced with intergrown orthopyroxene, magnetite and pleonaste. Reflected light.

Since plagioclase and olivine are abundant and no garnets have been found in the Rymmen gabbro, the upper limit is less than 10 kbar.

Temperature estimates of corona formation in the Rymmen gabbro using the amphibole-plagioclase geothermometer of Holland and Blundy (1994) give consistent temperatures of around 800 ± 30°C at 6–10 kbar. This is in accordance with the results of Whitney and McLelland (1973) from the Adirondack Region, USA. The amphibole-plagioclase geothermometer applied to the magmatic amphibole results in temperatures of 865 ± 35°C at 6–10 kbar. The two-pyroxene geothermometers of Wood and Banno (1973), Wells (1977), and Powell (1978) give temperatures from 930 to 1065°C using the magmatic orthopyroxene and clinopyroxene.

Griffin and Heier (1973) showed that the formation of coronas is favoured by slow cooling at depth. Schematic relations between nucleation rate, initial growth rate, and temperature under isobaric cooling, based on the experimental work of Green and Ringwood (1967), were used. The growth rate maximum for 8 kbar corresponds to a temperature of around 850°C (Griffin and Heier, 1973, Fig. 4). The coronas used were anhydrous, where clinopyroxene formed instead of amphibole.

Orthopyroxene-magnetite-pleonaste symplectites

P–*T* conditions of formation of the orthopyroxene-magnetite-pleonaste symplectites in the Rymmen gabbro are set by the estimates above, since stratigraphically the Fe-Ti rich zone is positioned between rocks that feature kelyphytic structures and both textures are considered to have developed during the same event. Other *P*–*T*-estimates of similar symplectites (Zeck *et al.*, 1982; Barton and Van Gaans, 1988) are not considered valid in this investigation.

Symplectites between plagioclase and magnetite/ilmenite

Fe-Ti oxide geothermometry (Ghiorso and Sack, 1991) results in low temperatures, between 270 and 450°C, showing the continued re-equilibration of the Fe-Ti oxides in gabbroic rocks.

Clinopyroxene-hornblende-plagioclase-quartz geobarometry on the Rymmen gabbro

The program Tweequ (Berman, 1991) was used on magmatic mineral assemblages from samples

TABLE 4. Symplectitic rim analyses in kelyphytic coronas

Sample	95585	95069	95069	95075	95608	95608	95606
Magn.	10000	10000	87000	10000	10000	10000	10000
Na_2O	0.23	1.51	1.55	1.18	1.11	n.d.	1.73
MgO	16.04	16.54	16.68	15.39	16.98	17.07	16.60
Al_2O_3	23.25	24.82	29.88	24.30	23.98	26.23	24.06
SiO_2	36.47	36.18	31.84	35.53	35.87	33.76	38.14
K_2O	0.03	n.d.	n.d.	0.26	0.03	n.d.	0.06
CaO	15.62	10.18	9.25	10.34	10.17	15.35	10.79
TiO_2	0.02	n.d.	n.d.	0.17	n.d.	n.d.	n.d.
Cr_2O_3	n.d.	n.d.	n.d.	n.d.	n.d.	n.d.	0.06
MnO	0.16	0.09	0.13	0.11	0.14	0.13	0.04
FeO	9.46	9.21	10.19	10.13	7.76	8.45	8.59
Sum	101.28	98.52	99.53	97.41	96.07	100.99	100.06
Mg'	75.1	76.2	74.5	73.1	79.6	78.3	77.5
Al/Si	0.75	0.81	1.11	0.81	0.79	0.92	0.74

n.d. = not detected.

in this study. The following solid solution models were used: Fuhrman and Lindsley (1988) for plagioclase, Newton (1983) for clinopyroxene and Mäder and Berman (1992) for hornblende. End-member properties given in Berman (1988) were used. The silica activity = 1. The Mg end-member equilibria ts+di+qtz = tr+an and prg+di+qtz = tr+an+ab of Mäder *et al.* (1994) at approximately 850°C (from plag-hbl in this study) gives pressures around 10–13 kbar. In Mäder *et al.* (1994) it is shown that the reaction ts+di+qtz = tr+an yields results 1–2 kbar too high compared with literature data at these pressures. None of the samples used in the calculation contain quartz. CIPW normative calculations performed on the samples used are silica saturated or are nepheline normative with nepheline less than 3 wt.%. This indicates that silica activity was below 1. Fig. 8.2. of Hughes (1982) shows silica activity as a function of temperature and mineralogy. If the En–Fo boundary is extrapolated from 900 to 850°C it will read around $-\log a_{SiO_2} = 0.3$ corresponding to a silica activity around 0.5. The silica activity is of great importance since the pressures are substantially lowered, down to 7 ± 0.5 kbar at a silica activity = 0.5 for the reaction ts+di+qtz = tr+an.

Al in amphibole geobarometry on the Rymmen gabbro

Amphibole interpreted as magmatic on petrographic criteria was used in the geobarometers of Hammarstrom and Zen (1986) and Johnson and Rutherford (1989). The geobarometer of Hammarstrom and Zen applied to the Rymmen gabbro gave a mean of 7 ± 1 kbar (1σ), range 5.1–11.0 and that of Johnson and Rutherford gave 5.5 ± 1 kbar (1σ), range 3.8–9.0 ($n = 126$).

TABLE 5. Orthopyroxene-magnetite-pleonaste symplectite analysis

Sample	Na_2O	MgO	Al_2O_3	SiO_2	K_2O	CaO	TiO_2	V_2O_5	MnO	FeO	Sum
95047 sym88	0.17	21.77	1.71	42.73	n.d.	0.14	0.34	0.19	0.43	36.90	104.38
95047 sym90	0.19	19.28	1.96	38.26	n.d.	0.12	0.28	0.29	0.43	43.44	104.21

n.d. = not detected.

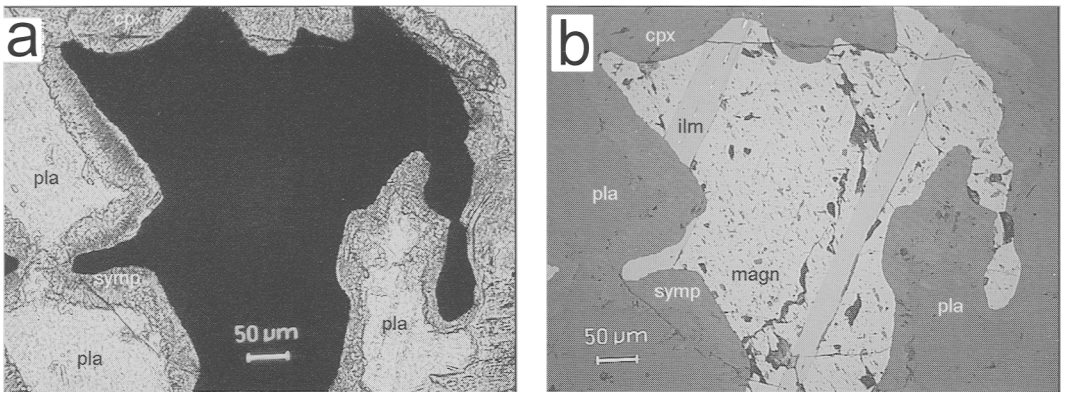

FIG. 4. In the Fe-Ti oxide rich part of the intrusion, symplectic coronas between Fe-Ti oxide and plagioclase is developed. (*a*) These are composed of amphibole and pleonaste. Plane-polarized light. (*b*) The magnetite has exsolution lamella of both hercynite and ilmenite. Reflected light.

However, these geobarometers are developed for a different set of minerals and the applicability in a gabbro is uncertain.

Discussion

Kelyphytic coronas

Disequilibrium between olivine and plagioclase has been forwarded as an explanation for the olivine-plagioclase reaction (e.g. Mongkoltip and Ashworth, 1983; Turner and Stüwe, 1992). The nature of the symplectite formation is demonstrated in Fig. 5, where a plagioclase is included in olivine. The plagioclase has reacted with the olivine and formed symplectite, but only in those parts that are close to fractures. Thus, from Fig. 5 one can draw the conclusion that sub-solidus fluid is responsible for the formation of the kelyphytic structure in the Rymmen gabbro. The cooling of the rock and development of fluids would result in coronas, reaction rims and symplectites under the pressure and temperature estimates given above. Fig. 5 also shows that fracturing of olivine and subsequent formation of symplectite within the olivine is an early process in the Rymmen gabbro and took place simultaneously with the formation of kelyphytic stuctures. The hydrous minerals, serpentine and chlorite, and magnetite found in the olivine developed after the corona formation at lower temperature. This is in contrast to Ashworth *et al.* (1992), who presumed that fracturing and formation of hydrous minerals took place after the corona formation in the Jotun Nappe, Norway. Carlson and Johnson (1991) showed that garnet–fluid reaction occurred along fractures that formed prior to a resorption event and resulted in two outboard layers of symplectite and magnetite.

The coronas in this study are interpreted as being the result of sub-solidus reactions, solid-

TABLE 6. Symplectite between plagioclase and Fe-Ti oxide analyses

Sample	Na_2O	MgO	Al_2O_3	SiO_2	K_2O	CaO	TiO_2	V_2O_5	MnO	FeO	Sum
95047 sym64	1.99	13.93	19.88	39.44	0.34	11.11	0.39	0.03	0.21	11.84	99.18
95047 sym85	0.22	13.11	22.54	37.09	0.16	10.61	0.04	0.01	0.22	12.83	96.84
95047 sym89	2.20	13.52	22.94	37.09	0.16	10.17	0.04	0.04	0.22	13.26	99.63

TABLE 7. Fe-Ti-Al oxide

Sample	95047 ilmexso65	95047 AlTiexso66	95047 pleoexso67	95047 magn68	95047 ilm69
MgO	1.18	0.28	8.42	0.22	1.38
Al_2O_3	0.17	65.32	33.44	0.52	0.29
SiO_2	0.07	0.22	0.10	0.12	0.14
CaO	0.04	0.01	0.02	0.04	0.13
TiO_2	52.49	18.16	0.50	0.81	53.73
V_2O_5	0.30	0.22	0.63	0.84	0.40
MnO	1.30	0.42	0.04	0.04	1.18
FeO	46.83	24.50	63.35	90.99	46.15
Sum	102.36	109.14	106.49	93.59	103.39
	ilmenite	titanian hercynite	hercynite	magnetite	ilmenite

TABLE 8. Amphibole-clinopyroxene reaction rim mineral analyses

Sample	95071 cpx30	95071 amp31 rim	95071 amp32	95071 cpx42	95071 amp43 rim	95071 amp44	95609 cpx8	95609 amp3 rim	95609 amp4
Na_2O	n.d.	n.d.	1.31	n.d.	0.51	1.16	n.d.	n.d.	0.60
MgO	15.68	18.77	13.61	15.63	18.02	13.91	16.31	20.51	16.00
Al_2O_3	3.61	3.42	13.58	3.91	4.86	13.27	2.65	4.31	12.14
SiO_2	52.50	55.64	45.16	52.53	55.43	45.27	53.72	54.03	44.51
K_2O	n.d.	n.d.	0.80	n.d.	n.d.	0.66	n.d.	0.09	0.82
CaO	23.01	13.35	12.63	21.25	13.44	12.61	24.69	13.44	12.68
TiO_2	0.41	0.09	1.50	0.30	0.17	1.40	0.56	0.34	1.59
Cr_2O_3	0.72	0.47	0.17	n.d.	0.68	0.22	0.33	0.06	0.58
MnO	0.10	0.10	0.19	0.26	0.11	0.16	0.20	0.08	0.12
FeO	5.26	7.44	9.92	5.44	7.27	9.76	3.71	5.07	7.89
NiO	n.d.	n.d.	n.d.	n.d.	n.d.	n.d.	0.09	0.05	0.13
Sum	101.29	99.28	98.88	99.33	100.48	98.40	102.26	97.99	97.07
Na	n.d.	n.d.	0.36	n.d.	0.13	0.32	n.d.	n.d.	0.17
Mg	0.85	3.86	2.90	0.86	3.70	2.97	0.87	4.24	3.45
Al	0.15	0.56	2.29	0.17	0.79	2.24	0.11	0.71	2.07
Si	1.90	7.68	6.46	1.93	7.62	6.49	1.92	7.50	6.44
K	n.d.	n.d.	0.15	n.d.	n.d.	0.12	n.d.	0.02	0.15
Ca	0.89	1.97	1.94	0.84	1.98	1.94	0.95	2.00	1.97
Ti	0.01	0.01	0.16	0.01	0.02	0.15	0.02	0.04	0.17
Cr	0.02	0.05	0.02	n.d.	0.07	0.02	0.01	0.01	0.07
Mn	0.00	0.01	0.02	0.01	0.01	0.02	0.01	0.01	0.01
Fe	0.16	0.86	1.19	0.17	0.84	1.17	0.11	0.59	0.95
Ni	n.d.	n.d.	n.d.	n.d.	n.d.	n.d.	0.00	0.01	0.02
Mg#	84.1	81.8	71.0	83.6	81.6	71.8	88.7	87.8	78.3
Wo	47	acti.	tsch.	45	acti.	tsch.	49	trem.	tsch.
En	44.5		hbl.	46		hbl.	45	hbl.	hbl.
Fs	8.5			9			6		

Formula on the basis of 6 resp. 23 oxygen for clinopyroxene and amphibole

n.d. = not detected.

TABLE 9. Pressure estimates for the olivine plagioclase reaction from the literature

Pressure estimate	8–9 kbar	Above 7 kbar	5–7 kbar	Less than 8 ± 1 kbar	6–10 kbar	Above 4– kbar	Above 6 kbar	7.5–8.5 kbar
Ref.	Griffin, 1971	Gill, 1981	Selverstone and Stern, 1983	Whitney and McLelland, 1983	Burns, 1985	Rivers and Mengel, 1988	Khan *et al.*, 1989	Dasgupta *et al.*, 1993

state replacement products that occurred during cooling from magmatic temperatures. The undeformed nature of the Rymmen gabbro and the volatile-rich content of its magma, evident from the magmatic amphibole within it, both imply that there is no need for a regional metamorphic event to explain the development of the coronas. This implies that the Rymmen gabbro was emplaced in the crust at a depth of 20–30 km (see P–T estimations above) with an overlying rock density corresponding to 3.8 km kbar^{-1} (Spear, 1993).

Grain-boundary diffusion controls the development of symplectite formation and nucleation sites, seen as nucleation on plagioclase facing olivine in Fig. 6. Access to late fluids could be a limiting factor of symplectite formation, as shown in Fig. 5, indicating that these coronas were formed in open systems (cf. Ashworth and Birdi, 1990; Carlson and Johnson, 1991). Aluminium mobility as a rate controlling factor for symplectite formation as suggested by Grant (1988) could in the Rymmen gabbro case be dependent on the access to late fluids.

Several types of spinel grains occur between symplectite and orthopyroxene in the kelyphytic coronas as shown in Fig. 2*c* and Table 3. Since the spinel grains differ in composition within a single corona and also occur elsewhere in the rock, they are interpreted as a primary mineral. This means that olivine and spinels crystallized earlier in the rock and the subsequent formation of coronas incorporated these spinel grains. The pleonaste grain could be a reaction product since its composition is similar to that of the spinel found in the symplectite. However, pleonaste grains occur in plagioclase that show no signs of reaction and are therefore interpreted as being primary.

Enstatite present in coronas is chemically different from the magmatic enstatite as it has higher alumina and calcium contents (Table 1). The Si/Al ratio of magmatic enstatite is almost constant, while corona enstatites in general have higher and variable Si/Al ratios. This difference indicates different genesis; equilibration at lower temperature or higher pressure, or different

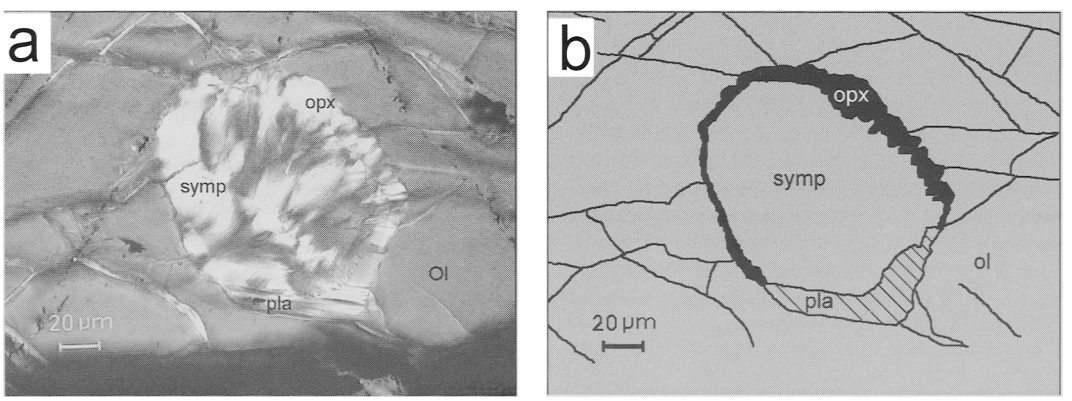

FIG. 5. Plagioclase inclusion in olivine. The plagioclase has reacted with the olivine and formed symplectite, but only in the part that is close to fractures. (*a*) Crossed polars. (*b*) Drawing based on a tracing of the photograph in 5*a*.

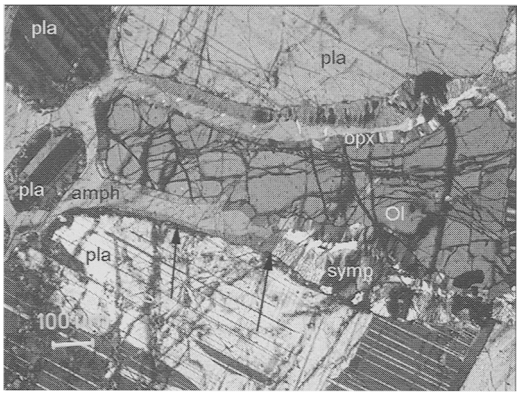

FIG. 6. Illustration of the diffusion controlled evolution of symplectite formation and nucleation sites. Grain-boundary diffusion is controlling the development, seen as nucleation on plagioclase indicated with arrow. Note that the symplectite stops abruptly, indicated with arrow. Crossed polars.

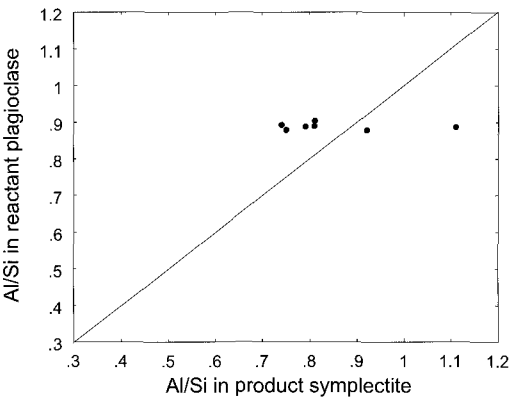

FIG. 7. Ratios of Al/Si for reacting plagioclase and produced symplectite are plotted against each other. Ashworth and Birdi (1990) used the relation to show the closure approximation for Al and Si.

partitioning when amphibole and spinel are present. Similar Mg # between coronitic and interstitial enstatite in a single sample may be due to Mg-Fe exchange during cooling (Ashworth, 1986). The magmatic reaction model of Joesten (cf. 1986*a,b*; Ashworth, 1986) is clearly not valid for the Rymmen gabbro since it is evident that the kelyphite formed in a solid-state replacement reaction.

Magmatic, interstitial amphibole has lower MgO and higher TiO_2 contents compared with coronitic amphibole in the same sample (Tables 1 and 2). The presence of tremolite in two coronas is probably due to a silica enrichment during deuteric reaction. The corona amphibole chemistry depends on the element supply rate (Trolliard *et al.*, 1988) and its low TiO_2 content indicates an aqueous fluid was present during its formation (e.g. Kogiso *et al.*, 1997).

The Al/Si ratios of reacting plagioclase and symplectite produced are plotted in Fig. 7. Ashworth and Birdi (1990) used the relation to show the closure approximation for Al and Si, i.e. relative immobility of these elements during olivine-plagioclase symplectite formation. Several samples plot off the equality line. Since symplectites are mixtures of minerals, the scatter of the analyses is probably due to the small area analysed and the fact that the proportions of the minerals are unknown. The analysis that plots furthest from the equality line, Al/Si = 1.11, had the smallest area analysed (~5 μm^2). Variation in the fluid flux, where the ratio amphibole/spinel formed in symplectite varies, might explain the variably open system (cf. Ashworth and Birdi, 1990; Ashworth and Sheplev, 1997) behaviour in the Rymmen gabbro.

Orthopyroxene-magnetite-pleonaste symplectites

Pegmatitic gabbro pods are evidence that fluids were enriched during differentiation. These fluids could have enhanced the formation of orthopyroxene-magnetite-pleonaste symplectites. The formation of these symplectites is probably controlled by grain-boundary diffusion and is a nonisochemical replacement (cf. Barton and Van Gaans, 1988; Barton *et al.*, 1991). Ambler and Ashley (1977) concluded that similar symplectites in the Wateranga layered mafic intrusion represent an eutectic-like texture developed during late magmatic crystallization.

Symplectites between plagioclase and magnetite/ilmenite

Plagioclase and a late stage aqueous fluid are suggested to react to form symplectite. The Fe-Ti oxide could act as a catalyst rather than being a reactant and the fluid transported Mg and Fe. Analyses of symplectites show low contents of titanium, although ilmenite is in direct contact with symplectite (Table 6). Since Ti is not easily transported in aqueous fluid (e.g. Kogiso *et al.*, 1997), this and the above implies that the fluid was aqueous. This is in strong contrast to coronas between ilmenite and plagioclase studied by Mall

and Sharma (1988) where Ti-rich phases were produced. Those that White and Clarke (1997) studied produced titaniferous biotite and garnet; still they concluded that the ilmenite mostly acted as a catalyst. Alternatively the magnetite/ilmenite was a reactant and Ti was retained in the oxide.

Conclusions

The factor that was most important for development of kelyphytic structures in the Rymmen gabbro was access to a late deuteric fluid. It also requires that olivine and plagioclase must be close to each other.

$P-T$ conditions of kelyphytic structure formation in the Rymmen gabbro were 800 ± 30°C at 6–8 kbar.

Late deuteric fluids caused olivine replacement by intergrown orthopyroxene and magnetite in the Fe-Ti oxide rich part of the intrusion.

The thickness of the continental crust of TIB in the studied area was in excess of 20–30 km at *c.* 1.7 Ga, deduced from the estimated emplacement depth of the Rymmen gabbro in this study.

Acknowledgements

I thank Professor S.-Å. Larson and Dr D. Cornell for supervision, Dr K.A. Kornfält and Dr H. Wikman at the Swedish Geological Survey (SGU) for support and encouragement. A review by J.R Ashworth improved this manuscript. This work benefited from financial support by SGU grant 03970/94 to D. Cornell.

References

Allan, J.F., Sack, R.O. and Batiza, R. (1988) Cr-rich spinels as petrogenetic indicators: MORB-type lavas from the Lamont seamount chain, eastern Pacific. *Amer. Mineral.*, **73**, 741–53.

Ambler, E.P. and Ashley, P.M. (1977) Vermicular orthopyroxene-magnetite symplectites from the Wateranga layered mafic intrusion, Queensland, Australia. *Lithos*, **10**, 163–72.

Ashworth, J.R. (1986) The role of magmatic reaction, diffusion and annealing in the evolution of coronitic microstructure in troctolitic gabbro from Risör, Norway: a discussion. *Mineral. Mag.*, **50**, 469–73.

Ashworth, J.R. and Birdi, J.J. (1990) Diffusion modelling of coronas around olivine in an open system. *Geochim. Cosmochim. Acta*, **54**, 2389–401.

Ashworth, J.R. and Sheplev, V.S. (1997) Diffusion modelling of metamorphic layered coronas with stability criterion and consideration of affinity. *Geochim. Cosmochim. Acta*, **61**, 3671–89.

Ashworth, J.R., Birdi, J.J. and Emmet, T.F. (1992) A complex corona between olivine and plagioclase from the Jotun Nappe, Norway, and the diffusion modelling of multimineralic layers. *Mineral. Mag.*, **56**, 511–25.

Barton, M., Sheets, J.M., Lee, W.E. and van Gaans, C. (1991) Occurrence of low-Ca clinopyroxene and the role of deformation in the formation of pyroxene - Fe-Ti oxide symplectites. *Contrib. Mineral. Petrol.*, **108**, 181–95.

Barton, M. and Van Gaans, C. (1988) Formation of orthopyroxene-Fe-Ti oxide symplectites in Precambrian intrusives, Rogaland, southwestern Norway. *Amer. Mineral.*, **73**, 1046–59.

Berman, R.G. (1988) Internally-consistent thermodynamic data for stoichiometric minerals in the system Na_2O-K_2O-CaO-MgO-FeO-Fe_2O_3-Al_2O_3-SiO_2-TiO_2-H_2O-CO_2. *J. Petrol.*, **29**, 445–522.

Berman, R.G. (1991) Thermobarometry using multi-equilibrium calculations: a new technique with petrologic applications. *Canad. Mineral.*, **29**, 833–55.

Burns, L.E. (1985) The Border Ranges ultramafic and mafic complex, south-central Alaska: cumulate fractionates of island-arc volcanics. *Canad. J. Earth Sci.*, **22**, 1020–38.

Carlson, W.D. and Johnson, C.D. (1991) Coronal reaction textures in garnet amphibolites of the Llano Uplift. *Amer. Mineral.*, **76**, 756–72.

Claeson, D. and Larson, S.Å. (1996) The Rymmen gabbro, a layered mafic intrusion from the Transscandinavian Igneous Belt, southern Sweden (abstract). *GFF, Jubilee Issue*, **118**, A 12.

Dasgupta, S., Sengupta, P., Mondal, A. and Fukuoka, M. (1993) Mineral chemistry and reaction textures in metabasites from the Eastern Ghats belt, India and their implications. *Mineral. Mag.*, **57**, 113–20.

Della-Pasqua, F.N., Kamenetsky, V.S., Gasparon, M., Crawford, A.J. and Varne, R. (1995) Al-rich spinel in primitive arc volcanics. *Mineral. Petrol.*, **53**, 1–26.

Fuhrman, M.L. and Lindsley, D.H. (1988) Ternary-feldspar modeling and thermometry. *Amer. Mineral.*, **73**, 201–16.

Gaál, G. and Gorbatschev, R. (1987) An Outline of the Precambrian Evolution of the Baltic Shield. *Precamb. Res.*, **35**, 15–52.

Ghiorso, M.S. and Sack, R.O. (1991) Fe-Ti oxide geothermometry: thermodynamic formulation and the estimation of intensive variables in silicic magmas. *Contrib. Mineral. Petrol.*, **108**, 485–510.

Gill, J.B. (1981) *Orogenic Andesites and Plate Tectonics*. Springer-Verlag, p. 204.

Gorbatschev, R. (1980) The Precambrian development

of southern Sweden. *Geol. För. Stockh. Förh.*, **102**, 129–36.

Gorbatschev, R. and Bogdanova, S. (1993) Frontiers in the Baltic Shield. *Precamb. Res.*, **64**, 3–21.

Grant, S.M. (1988) Diffusion models for corona formation in metagabbros from the Western Grenville Province, Canada. *Contrib. Mineral. Petrol.*, **98**, 49–63.

Green, D.H. and Ringwood, A.E. (1967) An experimental investigation of the gabbro to eclogite transformation and its petrological implications. *Geochim. Cosmochim. Acta*, **31**, 767–833.

Griffin, W.L. (1971) Genesis of Coronas in Anorthosites of the Upper Jotun Nappe, Indre Sogn, Norway. *J. Petrol.*, **12**, 219–43.

Griffin, W.L. and Heier, K.S. (1973) Petrological implications of some corona structures. *Lithos*, **6**, 315–35.

Hammarstrom, J.M. and Zen, E. (1986) Aluminium in hornblende: An empirical igneous geobarometer. *Amer. Mineral.*, **71**, 1297–313.

Holland, T. and Blundy, J. (1994) Non-ideal interactions in calcic amphiboles and their bearing on amphibole-plagioclase thermometry. *Contrib. Mineral. Petrol.*, **116**, 433–47.

Hughes, C.J. (1982) *Igneous Petrology, Developments in Petrology 7*, Elsevier, p. 258.

Joesten, R. (1986*a*) The role of magmatic reaction, diffusion and annealing in the evolution of coronitic microstructure in troctolitic gabbro from Risör, Norway. *Mineral. Mag.*, **50**, 441–67.

Joesten, R. (1986*b*) Reply. *Mineral. Mag.*, **50**, 474–9.

Johnson, M.C. and Rutherford, M.J. (1989) Experimental calibration of the aluminium-in-hornblende geobarometer with application to Long Valley caldera (California) volcanic rocks. *Geology*, **17**, 837–41.

Kamenetsky, V. and Clocchiatti, R. (1996) Primitive magmatism of Mt. Etna: insights from mineralogy and melt inclusions. *Earth Planet. Sci. Lett.*, **140**, 553–72.

Khan, M.A., Jan, M.Q., Windley, B.F., Tarney, J. and Thirlwall, M.F. (1989) The Chilas Mafic-Ultramafic Igneous Complex; The root of the Kohistan Island Arc in the Himalaya of northern Pakistan. *Geol. Soc. Amer. Special Paper*, **232**, 75–94.

Kogiso, T., Tatsumi, Y. and Nakano, S. (1997) Trace element transport during dehydration processes in the subducted oceanic crust: 1. Experiments and implications for the origin of ocean island basalts. *Earth Planet. Sci. Lett.*, **148**, 193–205.

Mäder, U.K. and Berman, R.G. (1992) Amphibole thermobarometry: a thermodynamic approach. *Current Research, Part E, Geological Survey of Canada, Paper 92-1E*, p. 393–400.

Mäder, U.K., Percival, J.A. and Berman, R.G. (1994) Thermobarometry of garnet-clinopyroxene-hornblende granulites from the Kapuskasing structural zone. *Canad. J. Earth Sci.*, **31**, 1134–45.

Mall, A.P. and Sharma, R.S. (1988) Coronas in olivine metagabbros from the Proterozoic Chotanagpur terrain at Mathurapur, Bihar, India. *Lithos*, **21**, 291–300.

Mongkoltip, P. and Ashworth, J.R. (1983) Quantitative Estimation of an Open-system Symplectite-forming Reaction: Restricted Diffusion of Al and Si in Coronas around Olivine. *J. Petrol.*, **24**, 635–61.

Natland, J.H. (1989) Partial melting of a lithologically heterogenous mantle: inferences from crystallization histories of magnesian abyssal tholeiites from the Siqueiros Fracture Zone. In *Magmatism in Ocean Basins* (A.D. Saunders and M.J. Norry, eds.), Geol. Soc. London Spec. Publ. **42**, 41–70.

Newton, R.C. (1983) Geobarometry of high-grade metamorphic rocks. *Amer. J. Sci.*, **283-A**, 1–28.

Passchier, C.W. and Trouw, R.A.J. (1996) *Microtectonics*. Springer-Verlag, 190–2.

Powell, R. (1978) The thermodynamics of pyroxene geotherms. *Phil. Trans. R. Soc. Lond. A*, **288**, 457–69.

Rivers, T. and Mengel, F.C. (1988) Contrasting assemblages and petrogenetic evolution of corona and noncorona gabbros in the Grenville Province of western Labrador. *Canad. J. Earth Sci.*, **25**, 1629–48.

Selverstone, J. and Stern, C.R. (1983) Petrochemistry and recrystallization history of granulite xenoliths from the Pali-Aike volcanic field, Chile. *Amer. Mineral.*, **68**, 1102–12.

Spear, F.S. (1993) Metamorphic Phase Equilibria and Pressure-Temperature-Time Paths. *Monograph Series, Mineral. Soc. Amer.*, p. 8.

Tindle, A.G. and Webb, P.C. (1994) PROBE-AMPH - a spreadsheet program to classify microprobe-derived amphibole analyses. *Computers & Geosci.*, **20**, 1201–28.

Trolliard, G., Boudeulle, M., Lardeaux, J.M. and Potdevin, J.L. (1988) Contrasted Modes of Amphibole Development in Coronitic Metagabbros: a TEM Investigation. *Phys. Chem. Minerals*, **16**, 130–9.

Turner, S.P. and Stüwe, K. (1992) Low-pressure corona textures between olivine and plagioclase in unmetamorphosed gabbros from Black Hill, South Australia. *Mineral. Mag.*, **56**, 503–9.

Turnock, A.C. and Eugster, H.P. (1962) Fe-Al Oxides: Phase Relationships below 1,000°C. *J. Petrol.*, **3**, 533–65.

Wells, P.R.A. (1977) Pyroxene Thermometry in Simple and Complex Systems. *Contrib. Mineral. Petrol.*, **62**, 129–39.

White, R.W. and Clarke, G.L. (1997) The Role of

Deformation in Aiding Recrystallization: an Example from a High-pressure Shear Zone, Central Australia. *J. Petrol.*, **38**, 1307–29.

Whitney, P.R. and McLelland, J.M. (1973) Origin of Coronas in Metagabbros of the Adirondack Mts., N. Y. *Contrib. Mineral. Petrol.*, **39**, 81–98.

Whitney, P.R. and McLelland, J.M. (1983) Origin of Biotite-Hornblende-Garnet Coronas Between Oxides and Plagioclase in Olivine Metagabbros, Adirondack Region, New York. *Contrib. Mineral. Petrol.*, **82**, 34–41.

Wood, B.J. and Banno, S. (1973) Garnet-orthopyroxene and orthopyroxene-clinopyroxene relationships in simple and complex systems. *Contrib. Mineral. Petrol.*, **42**, 109–24.

Zeck, H.P., Shenouda, H.H., Rønsbo, J.G. and Poorter, R.P.E. (1982) Hypersthene-ilmenite(/magnetite) symplectites in coronitic olivine-gabbronorites. *Lithos*, **15**, 173–82.

[*Manuscript received 12 December 1997: revised 10 March 1998*]